Ultra-Wideband Transmission with Polarization Diversity for Constant QoS in Short-Range Communications

E. Del Re, F. Argenti, T. Bianchi, L. Mucchi and L. S. Ronga
University of Florence
Department of Electronics and Telecommunications
via S. Marta, 3 I-50139 Firenze, Italy
Email: mucchi@lenst.det.unifi.it
Phone: +390554796413
Fax: +390554796485
This work has been developed as part of the VICOM project (www.vicom-project.it).

***Abstract*— In this paper a multiband UWB signal with polarization diversity is considered in order to maintain as constant as possibile the performance (and consequently the QoS) of a short range communication link.**

I. Introduction

Recently, a different concept of UWB signal emerged [1][2][3]. Instead of transmitting single impulses occupying a large bandwidth, the available spectrum is divided into several bands that can be accessed separately by a single or multiple users. Due to FCC definition, each band must be at least 500 MHz. Usually, a number of bands between 3 and 10 is taken into consideration. This method, referred to as *multiband UWB*, has several advantages with respect to *impulse radio UWB*. A flat PSD can be accomplished in each band, so that higher power can be conveyed into the channel with respect to impulse-based UWB. Choosing proper positions of the bands allows regional regulation constraint on spectrum occupancy to be met. Also from an implementation point of view, the multiband approach is attracting since less stringent requirements can be imposed on the ADC sampling rate and dynamic range, so that a software-defined receiver becomes feasible. Different combinations of CDMA and OFDM have been proposed for fully exploiting the 500 MHz band and several band-hopping methods have been foreseen to allow several users to access the channel as well several piconets to coexist.

Another important aspect of UWB systems is antenna technology and design related to minimum space occupancy and portability as well as space diversity exploitation [4][5]. Critical points in antenna design are the required huge bandwidth and the trade-off between antenna gain, antenna dimensions and flatness of the antenna-to-antenna response [6]. More attention must be paid to the position of the transmitting and receiving antennas and their relative orientation since this influences the antenna-to-antenna frequency response. For transmission between several devices and a base station, more than one antenna can be foreseen at the base station, but only one, for dimension containment, at the portable devices. Exploiting such diversity is an important issue of UWB systems.

In this study, an UWB transmission system able to provide a fast, local-range, wireless connection on an unlicensed basis by using the same frequency spectrum assigned to other narrowband communication standards is considered. Several channel models have been presented in the literature [7][8][9], but only a few consider the distortion effect caused by a real UWB antenna.

Based on the observation that the antenna-to-antenna frequency response strongly depends on the mutual orientation, a technique using two transmitting antennas with orthogonal orientation to create diversity in the received UWB signal is proposed. The receiver is equipped with a single antenna whose orientation and position are arbitrary within the coverage area, thus resulting in a special case of a 2:1 MIMO system. Space-time[1] encoding is used at the transmitter to exploit polarization diversity without increasing the signal bandwidth [10]. The performance of different multiple access schemes for the downlink is investigated. It will be demonstrated that the proposed system allows reliable detection independently of the receiving antenna orientation and a uniform coverage of the indoor area.

II. Antenna Issues and Polarization Diversity

The study and design of UWB antennas has a key role in assessing the overall performance of a communication system. In this section, the specific antenna considered for our analysis is described. The antenna has been designed for impulse radio UWB systems, but can be used also for our multiband UWB system.

The complete antenna design and analysis is described in [6]. It is a slot antenna, having a length of approximately six inches. The shape of the antenna is shown in Figure II. Although a particular type of antenna is considered, the proposed method can be applied to any antenna shape. In [6], a tool for achieving the three-dimensional radiation pattern of the antenna is presented. Once the relative positions and orientations of the receiving and transmitting antennas are given, the antenna-to-antenna transfer function, computed on a preassigned frequency grid, can be evaluated. As it will be shown, these transfer functions are strongly dependent on the relative orientations of the antennas.

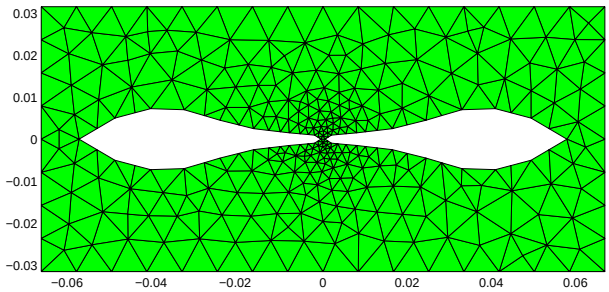

Fig. 1. Shape of the slot antenna designed for UWB communications (the dimensions are in meters).

[1]The term polarization-time would be more appropriate in this context. Here, we use the term space-time since it is customary in multiple antenna systems.

To avoid performance loss due to the orientation-variant radiation pattern, two antennas with orthogonal orientation at the transmission side is used. It will be demonstrated that such a system is able to deliver a sufficiently high level of signal *independently of the orientation of the receiving antenna*.

In Figure II, the specific indoor environment used to simulate the proposed system is shown. It sketches a quite large environment ($16 \times 16 \times 7$ meters), with a staircase leading to an intermediate floor. The two base station antennas, with orthogonal orientation, are placed on the ceiling of the room. Seven different possible locations and orientations of the portable UWB device are shown. In Fig. 3, the amplitude antenna-to-antenna transfer functions evaluated for each position and for each transmitting antenna (denoted with H and V polarization) are given. As can be seen, a common trend for all polarizations and all locations is that the amplitude response decreases with frequency, so that the highest frequency bands are expected to yield the main contribution to the total bit error rate.

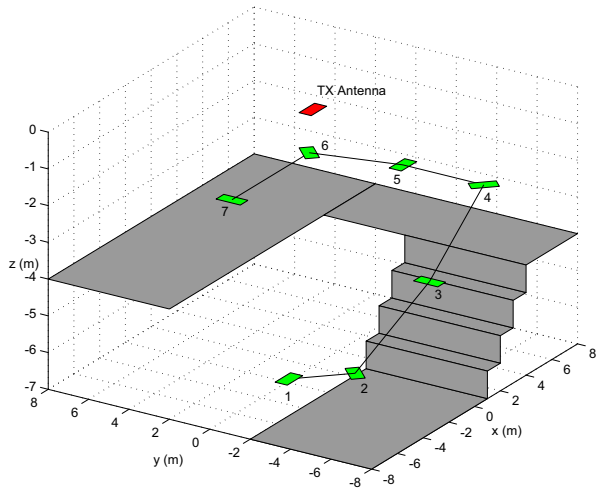

Fig. 2. Scheme of the indoor environment. The position of the base station antennas and seven different possible locations and orientations of the UWB device are shown.

Diversity can be created in the time, frequency or space domain to combat negative effects of the channel due to fading [11]. Also cross-polarized antennas can be used to increase the diversity order at the receiver [12][13][14][15]. In a space diversity scheme, i.e., based on an antenna separation equal to ten times the wavelength, a uniform coverage is not guaranteed with real antennas due to the frequency distortion induced by orientation. With polarization diversity this problem can be avoided.

But, diversity may decrease the resources available for user data transmission. Recently, space-time coding methods have been proposed to exploit diversity without wasting system resources. In this study, Alamouti's scheme [16], a well-known two-branches space-time block coding (STBC) method, is considered. It allows two coded symbols to be transmitted in two consecutive time intervals over two channels that, in this case, are related to the orthogonally oriented antennas. Alamouti's method is now briefly reviewed. Let s_0 and s_1 be the complex symbols to be transmitted in the consecutive time intervals $(0, T)$ and $(T, 2T)$. The symbols transmitted over the antennas in the time intervals $\{(0, T), (T, 2T), \ldots\}$, are

$$\text{Antenna V:} \quad \{c_{V1}, c_{V2}, \ldots\} = \{s_0, -s_1^*, \ldots\}$$

$$\text{Antenna H:} \quad \{c_{H1}, c_{H2}, \ldots\} = \{s_1, s_0^*, \ldots\}$$

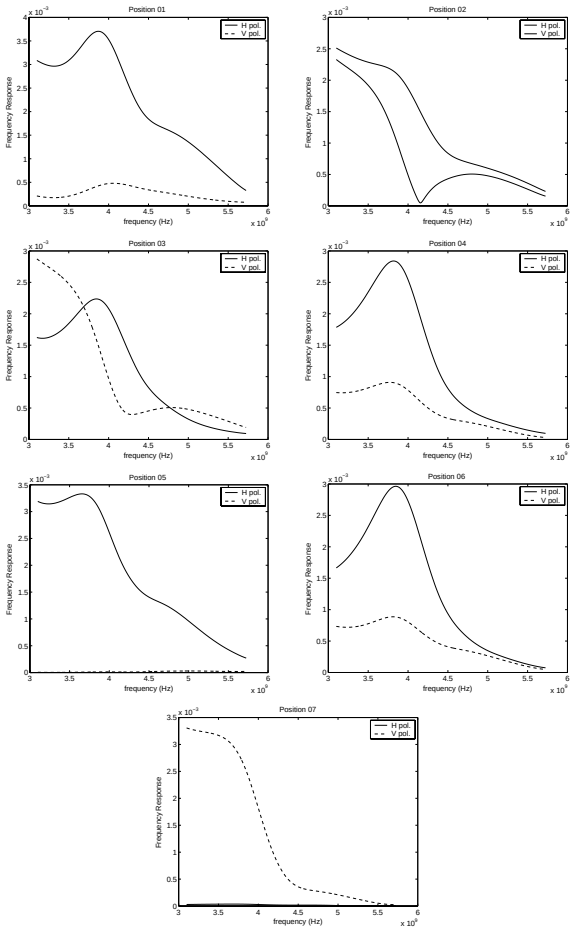

Fig. 3. Amplitude transfer functions in the different positions of the UWB device within the room.

Let h_H and h_V be the complex gain introduced by the channel in the links from the H and V antenna to the receiver. In this scheme, it is assumed that the channel coefficients do not vary within the period $(0, 2T)$. Hence, the received signal sequence $\{r_0, r_1, \ldots\}$ is

$$\{r_0, r_1, \ldots\} = \{s_0 h_V + s_1 h_H + n_0, -s_1^* h_V + s_0^* h_H + n_1, \ldots\}$$

where n_0 and n_1 are the AWGN contribution. The space-time decoder, which has knowledge of the channel status, builds two decision variables by combining the received symbols as follows

$$\begin{aligned}\{\hat{s}_0, \hat{s}_1, \ldots\} &= \{r_0 h_V^* + r_1^* h_H, r_0 h_H^* - r_1^* h_V, \ldots\} \\ &= \{s_0(|h_V|^2 + |h_H|^2) + n_0 h_V^* + n_1^* h_H, \\ &\qquad s_1(|h_V|^2 + |h_H|^2) + n_0 h_H^* - n_1^* h_V, \ldots\}\end{aligned}$$

As can be seen, a factor two of diversity gain is achieved.

III. System model: Multiband UWB

The proposed system uses a multiband approach to generate the UWB signal. It will be assumed that M bands can be accessed by the users or the devices connected to the system. According to the FCC recommendations, each band must be at least W Hz wide, where $W > 500$ MHz. The boundary and center frequencies of the proposed UWB system, for which we have chosen $M = 4$, are shown in Table I.

The multiband approach allows the channel to be shared by the different users by means of frequency division multiplex (FDM).

TABLE I
BOUNDARY AND CENTER FREQUENCIES (GHZ) OF THE PROPOSED UWB SYSTEM.

Band	Low	Center	High
1	3.1	3.35	3.6
2	3.725	3.975	4.225
3	4.35	4.6	4.85
4	5.225	5.475	5.725

Each band is divided into temporal slots and accessed by means of time division multiplex (TDM). Note that a user device can access contemporarily more than one band only if it disposes of a multi-carrier demodulator. Due to the large frequency width, multipath propagation affects the reception of signals in each band. Orthogonal frequency division multiplex (OFDM) has been proposed to combat channel degradation due to a frequency selective channel [17][18]. The transmitted symbol in each time/frequency tile, created by the mixed FDM/TDM multiple access, is obtained by applying OFDM to a set of user information bits. Since OFDM creates a further splitting of the available spectrum, several choices for assigning frequency bins (belonging, eventually, to different bands) to active users can be considered. The different strategies will be discussed in the following subsection.

A. Multiple Access in Multiband UWB

Assume that each band is divided into N subcarriers. In the proposed system $N = 128$ has been assumed. Hence, MN subcarriers are available to be assigned to the total number, say K, of active users. For the sake of simplicity, a progressive index spanning all the subcarriers, even if they belong to different bands, is used. Hence the nth subcarrier, $n = 0, 1, \ldots, MN-1$, has the frequency

$$f_n = f_{q,low} + \Delta f\, p$$

where $n = q\,N + p$, $f_{q,low}$ is the lower bound frequency assigned to the qth band, and $\Delta f = W/N$ is the subcarrier spacing.

It is assumed that each subcarrier is exclusively assigned to each user, i.e., it can not be shared between two, or more, users. Let

$$I(k,l) = \{i_{k,l,m}, m = 0, 1, \ldots, M_I - 1\}, \quad k = 0, 1, \ldots, K-1,\ l = 0, 1, 2, \ldots \tag{1}$$

be the subset of carriers assigned to the kth user in the lth symbol time. The number of carriers M_I assigned to each user in each symbol time depends on the type of multiple access that is used.

B. Signal model

Let $d_{k,n}^{(l)}$ be the data symbol transmitted by the kth user in the lth symbol time over the nth subcarrier. In the following, it will be assumed that $d_{k,n}^{(l)}$ belongs to a given constellation of symbols. After Alamouti's STBC, two sequences, $\{c_{H,k,n}^{(l)}\}$ and $\{c_{V,k,n}^{(l)}\}$, are created and transmitted over the H and V antenna. By using the definitions given in the previous section, we have

$$s_{X,k,n}^{(l)}(t) = c_{X,k,n}^{(l)} e^{j2\pi f_n t} \tag{2}$$

for $t \in [lT, (l+1)T]$, where T is the symbol duration time and X denotes either the H or the V antenna. Hence, the signal transmitted over the qth band by the X antenna is

$$S_{X,q}^{(l)}(t) = \sum_{k=0}^{K-1} \sum_{n \in I(k,l), n=qN}^{(q+1)N-1} c_{X,k,n}^{(l)} e^{j2\pi f_n t} \tag{3}$$

Consider now the effect of the channel on the transmitted signal. It can be modeled as the convolution of the antenna-to-antenna transfer function with a random process taking into account different channel characteristics (multipath, fading, time variability, etc.). The slicing of the spectrum into several narrow subbands makes the channel in each subcarrier flat. Assuming a slow motion of the mobile user, the effect of the channel on the nth subcarrier within the lth time interval is modeled as a complex constant that will be denoted as

$$h_{X,n}^{(l)} = \alpha_{X,n}^{(l)} e^{j\phi_{X,n}^{(l)}} \tag{4}$$

A description of the channel model and of the statistics assumed to derive the variable $h_{X,n}^{(l)}$ are given in the next section.

The signal received by the user, equipped with a single antenna, in the nth band and in the lth symbol time interval is given by

$$\begin{aligned} R^{(l)}(t) &= \sum_{q=0}^{M-1} S_{H,q}^{(l)}(t) + S_{V,q}^{(l)}(t) \\ &= \sum_{k=0}^{K-1} \sum_{n \in I(k,l)} \alpha_{H,n}^{(l)} e^{j\phi_{H,n}^{(l)}} c_{H,k,n}^{(l)} e^{j2\pi f_n t} \\ &\quad + \sum_{k=0}^{K-1} \sum_{n \in I(k,l)} \alpha_{V,n}^{(l)} e^{j\phi_{V,n}^{(l)}} c_{V,k,n}^{(l)} e^{j2\pi f_n t} + w(t) \end{aligned} \tag{5}$$

where $w(t)$ is AWGN. To extract the information delivered by the nth subcarrier, the receiver performs the correlation with $e^{-j2\pi f_n t}$, i.e.,

$$\begin{aligned} r_{k,n}^{(l)} &= \int_{lT}^{(l+1)T} R_m^{(l)}(t) e^{-j2\pi f_n t} dt = \\ &= \alpha_{H,n}^{(l)} e^{j\phi_{H,n}^{(l)}} c_{H,k,n}^{(l)} + \alpha_{V,n}^{(l)} e^{j\phi_{V,n}^{(l)}} c_{V,k,n}^{(l)} + w_{k,n}^{(l)} \end{aligned} \tag{6}$$

By applying Alamouti's decoder to two consecutive received symbols we have

$$\begin{aligned} \hat{d}_{k,n}^{(l)} &= r_{k,n}^{(l)} \alpha_{V,n}^{(l)} e^{-j\phi_{V,n}^{(l)}} + (r_{k,n}^{(l+1)})^* \alpha_{H,n}^{(l)} e^{j\phi_{H,n}^{(l)}} \\ \hat{d}_{k,n}^{(l+1)} &= r_{k,n}^{(l)} \alpha_{H,n}^{(l)} e^{-j\phi_{H,n}^{(l)}} - (r_{k,n}^{(l+1)})^* \alpha_{V,n}^{(l)} e^{j\phi_{V,n}^{(l)}} \end{aligned} \tag{7}$$

and by using (6) into (7) we have

$$\begin{aligned} \hat{d}_{k,n}^{(l)} &= ((\alpha_{V,n}^{(l)})^2 + (\alpha_{H,n}^{(l)})^2) d_{k,n}^{(l)} + \\ &+ w_{k,n}^{(l)} \alpha_{V,n}^{(l)} e^{-j\phi_{V,n}^{(l)}} + (w_{k,n}^{(l+1)})^* \alpha_{H,n}^{(l)} e^{j\phi_{H,n}^{(l)}} \\ \hat{d}_{k,n}^{(l+1)} &= ((\alpha_{V,n}^{(l)})^2 + (\alpha_{H,n}^{(l)})^2) d_{k,n}^{(l+1)} + \\ &+ w_{k,n}^{(l)} \alpha_{H,n}^{(l)} e^{-j\phi_{H,n}^{(l)}} - (w_{k,n}^{(l+1)})^* \alpha_{V,n}^{(l)} e^{j\phi_{V,n}^{(l)}} \end{aligned} \tag{8}$$

IV. THE UWB CHANNEL

Models for describing the effect of the channel are usually extracted from sets of measurements conducted in different indoor/outdoor environments [7][8][9][19]. The set of measurement should be sufficiently large so that a general model, able to capture the main characteristics of the channel, can be derived.

The model used for narrowband signals is not valid for UWB signals. The time resolution of the system is so high that the number of paths impinging the receiver antenna in a time-resolution bin is not so large to justify the use of the central limit theorem. The IEEE 802.15.3a task group [20], aiming at defining a standard for a wireless interface based on UWB, has evaluated how a certain number of indoor wireless channel models fitted the set of UWB channel measurements. Among available models, that of Saleh and

Valenzuela [19] has been found particularly suitable to describe the behavior of the UWB channel.

Based on this model and on a set of propagation measurements, Foerster *et al.* [8] introduced a modified model for UWB signals. The impulse response of the channel is assumed equal to

$$h(t) = Y \sum_{j=0}^{J} \sum_{p=0}^{P} \alpha_{j,p} \delta(t - T_j - \tau_{j,p}) \tag{9}$$

where T_j is the arrival time of the first ray of the jth cluster, $\tau_{j,p}$ is the arrival time of the pth path within the jth cluster (measured starting from the arrival of the first ray), $\alpha_{j,p}$ is the complex gain of each path, Y models the shadowing of the link. The interarrival times between clusters ($T_j - T_{j-1}$) and the interarrival times between rays within a cluster ($\tau_{j,p} - \tau_{j,p-1}$) are exponentially distributed with arrival rates Λ and λ, respectively. The power delay profiles of clusters and of rays within a cluster are exponentially distributed with decay factors Γ and γ, respectively. The path complex gain can be written as $\alpha_{j,p} = \xi_j \beta_{j,p}$, where ξ_j and $\beta_{j,p}$ are distributed as log-normal random variables, that is $20 \log_{10} \xi_j$ and $20 \log_{10} \beta_{j,p}$ are normal random variables, i.e., $\mathcal{N}(0, \sigma_1^2)$ and $\mathcal{N}(0, \sigma_2^2)$, respectively. Hence, also $\alpha_{j,p}$ is log-normally distributed, that is $20 \log_{10} \alpha_{j,p}$ is $\mathcal{N}(\mu_{j,p}, \sigma_1^2 + \sigma_2^2)$, where $\mu_{j,p}$ is computed by normalizing the path energy with respect to the first arrived path energy. This normalization takes into account the power delay profiles with decay factors Γ and γ and the values of the realization of the interarrival times (see [8] for more details). Finally, Y is a log-normal distributed shadowing, that is $20 \log_{10} Y$ is $\mathcal{N}(0, \sigma_Y^2)$.

In the present study, a mixed deterministic/statistic modeling of the channel is used.

It is assumed that a LOS link between the transmitter and the receiver exists. This link is modeled as a deterministic transfer function depending on the frequency as well as on the relative orientation of the transmitting and receiving antennas. The seven positions and orientations sketched in Fig. II, whose transfer functions are plotted in Fig. 3, have been taken into consideration in the simulations.

This deterministic model, however, does not include the several echoes received after reflections and diffraction around objects in the room, i.e., the non-LOS (NLOS) part of the received signal. Dealing such echoes in a deterministic way affects the generality of the environment and its modeling. Hence, a statistic modeling for this NLOS component has been considered. For this purpose, the model described in [8] and previously reviewed has been used. The values of the parameters of the models that have been used in the simulations are taken from [8] and are reported in Table II. It should be noted that, due to the nature of the UWB transmission, the parameters of this model do not refer to a baseband representation.

The LOS and the NLOS components are linearly combined according to a parameter θ that allows us to vary the percentage of energy deriving from the LOS component. Let $a_{X,n}$ be the transfer function of the LOS link from the X (either H or V) to the receiving antenna, measured at the nth subcarrier frequency. This function depends on the positions of the receiver and on the relative orientation of the transmitting/receiving antennas but does not depend on time. Samples of this function are plotted in Fig. 3. Moreover, let $g_{X,n}^{(l)}$ be a realization of the coefficients obtained from the NLOS model at the nth subcarrier frequency, valid for the X antenna link and at the lth symbol time. The coefficients $h_{X,n}^{(l)}$ used in Section III-B are given by

$$h_{X,n}^{(l)} = \sqrt{\theta}\ a_{X,n} + \sqrt{1-\theta}\ g_{X,n}^{(l)}\, b_n \tag{10}$$

The function b_n is the antenna-to-antenna transfer function when the transmit and receive antenna are favorably coupled and at a distance of three meters (the minimum distance in the walk depicted in Fig. II). This function has been introduced to simulate the reception of the NLOS component by our specific antenna system. In fact, it yields a frequency shaping to the NLOS component dependent on the antenna characteristics and similar to that encountered by the LOS component.

TABLE II
PARAMETERS OF THE CHANNEL MODEL

Λ	0.0667	[1/ns]
λ	2.1	[1/ns]
Γ	14	
γ	7.9	
σ_1	3.4	[dB]
σ_2	3.4	[dB]
σ_Y	3	[dB]

A feature that must also be considered for a realistic simulation of our system is the correlation between the signals transmitted from the two orthogonally disposed antennas. Since the correlation coefficient between the two channels depends on several factors, quite difficult to be modeled, in this study the two extreme cases, in which the channels, i.e., the variables $g_{H,n}^{(l)}$ and $g_{V,n}^{(l)}$, are either completely correlated or completely uncorrelated are considered. The experimental results will demonstrate that the proposed system yields a gain with respect to a single antenna system in both cases.

V. PROBABILITY OF ERROR

The probability of error of the UWB communication system depends on the signalling used and on the status of the channel. Since the multiband UWB communication link provides M macrobands, each one divided into N OFDM subcarriers, the probability of error for a single subcarrier is first analyzed. By assuming that a single antenna is used, either H or V, and that the modulation is binary antipodal, the expression for the error rate as a function of the received SNR $\gamma_{b,n}$ at the nth subcarrier is given by

$$P_2(\gamma_{b,n}^{(l)}) = Q\left(\sqrt{2\gamma_{b,n}^{(l)}}\right) \tag{11}$$

where

$$\gamma_{b,n}^{(l)} = |h_{X,n}^{(l)}|^2 \frac{E_b}{N_0} \tag{12}$$

and $h_{X,n}^{(l)}$ is the channel coefficient seen from the X antenna to the receiver at the generic nth subcarrier frequency, given in (10). This channel coefficient takes into account both the antenna orientation effect as well as the multipath nature of the UWB channel.

In the case of space-time transmit diversity with order two at the receiver, the probability of error measured at a single OFDM subcarrier is again given by $P_2(\gamma_{b,n}^{(l)})$ in (11) where now, however, $\gamma_{b,n}^{(l)}$ is given by

$$\gamma_{b,n}^{(l)} = (|h_{H,n}^{(l)}|^2 + |h_{V,n}^{(l)}|^2) \frac{E_b}{N_0} \tag{13}$$

This results is true if the channel coefficients from the two antennas are independent of each other and if they do not vary during two consecutive bit intervals.

The probability of error seen by the kth user of interest is the average over all the subcarriers. Let

$$\mathbf{\Omega}_k^{(l)} = [\gamma_{b,n_1}^{(l)}, \cdots, \gamma_{b,n_{M_I}}^{(l)}]^T,\ n_1, \cdots, n_{M_I} \in I(k,l) \tag{14}$$

be the vector of SNRs over the M_I subcarriers assigned to the kth user at the lth time interval. M_I and $I(k,l)$ are defined in Section III-A.

The desired probability of error is then given by

$$P_2(\mathbf{\Omega}_k^{(l)}) = \frac{1}{M_I} \sum_{n \in I(k,l)} P_2(\gamma_{b,n}^{(l)}) \tag{15}$$

In order to obtain the unconditional error probability, $P_2(\mathbf{\Omega}_k^{(l)})$ has to be averaged over the joint probability density function of $\mathbf{\Omega}_k^{(l)}$, i.e., the following integral has to be calculated[2]

$$P_2 = \int P_2(\mathbf{\Omega}_k^{(l)}) p(\mathbf{\Omega}_k^{(l)}) d\mathbf{\Omega}_k^{(l)} \tag{16}$$

Unfortunately, a closed form of the integral in (16) is not easy to achieve due to the complex formulation of the random variables $\gamma_{b,n}^{(l)}$ that depend instantaneously on the channel complex value $h_{X,n}^{(l)}$ seen between the transmitter and the receiver.

Due to the problems related to solving (16), a semi-analytical approach, based on Monte Carlo simulations, has been used to evaluate the total average probability of error. A set of channel coefficients $\{h_{X,n}^{(l)}\}$ for each antenna was generated, so that the (15) could be computed. Then, the total average probability of error P_2 is approximated by

$$\overline{P}_2 = \frac{1}{N_r} \sum_{z=1}^{N_r} P_2(\mathbf{\Omega}_{k,z}^{(l)}) \tag{17}$$

where $\mathbf{\Omega}_{k,z}^{(l)}$ is the zth realization of the vector $\mathbf{\Omega}_k^{(l)}$ and N_r is the number of Monte Carlo trials.

The numerical results are reported in the next section VI.

VI. Results

The performance of the proposed system has been evaluated by means of a semi-analytical approach. $N_r = 100$ independent realizations of the UWB channel model described in Section IV have been generated, considering all the seven positions and orientations reported in Section II. Hence, the conditional probability of error relative to each channel realization relying on the SNR expressed in (12) for the single-antenna case and on (13) for the polarization diversity case, respectively, was evaluated. Finally, the overall performance of the different systems by averaging the probability of error over the N_r channel realizations was obtained.

Four systems based on different antenna configurations and channel hypotheses are considered. The first two systems, denoted as *H Pol.* and *V Pol.*, refer to the cases in which only one of either the H or V antenna is employed at the transmitter. The name *HV Corr.* denotes the system using two antennas with orthogonal orientations and Alamouti's coding, assuming that the NLOS components of the two channels, i.e., $g_{H,n}^{(l)}$ and $g_{V,n}^{(l)}$, are completely correlated. Conversely, with *HV Ind.* an analogous two-antenna system, where $g_{H,n}^{(l)}$ and $g_{V,n}^{(l)}$ are completely uncorrelated, is denoted.

The results of simulations considering the TDM access scheme, described in Section III-A, are shown in Fig. 4. In this case, we suppose that LOS path carries the 80% of total transmitted power, i.e., $\theta = 0.8$. The error probability relative to each receiver position and orientation as well as the error probability obtained by averaging over all the seven positions are shown. As it can be seen, the proposed system gains almost 5dB in the average.

The performance of the single-antenna systems varies widely for the different receiver positions and antenna orientations as well as considering either the H or V antenna at the transmitter. The proposed polarization-diversity schemes allow us to achieve a performance very close to that of the "best" transmit antenna, i.e., the antenna showing the most favorable amplitude response with respect to the current receiver position and orientation. As a result, the average error probability of the polarization-diversity schemes outperforms that of both the *H Pol.* and the *V Pol.* schemes. Moreover, the behavior of the polarization-diversity scheme appears to be independent of the correlation between the NLOS components of the two channels. The diversity gain showed in the average performance is to be ascribed mainly to the different frequency responses due to the orthogonal orientations of the two transmit antennas. It is worth noting that this fact allows us to avoid any space separation between the two antennas.

[2]The dependence on the time index l is here dropped, because the probability of error is assumed not to be dependent on the instant of observation.

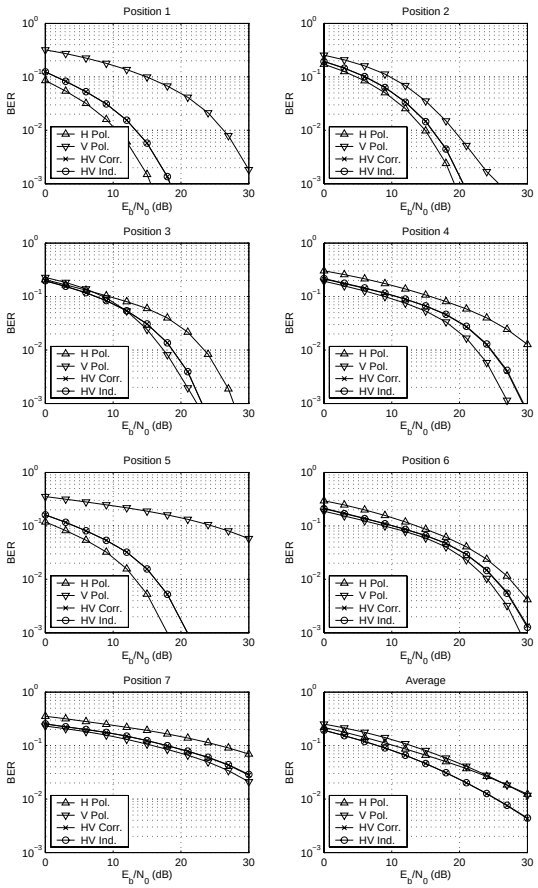

Fig. 4. Performance of single-antenna (*H pol.* and *V pol.*) and polarization-diversity (*HV corr.* and *HV ind.*) systems. The different positions/orientations described in Section II are considered. The right bottommost figure plots the average of the other curves. TDM access scheme with LOS carrying 80% of the total transmitted power has been used.

References

[1] UWB Multiband Coalition [Online]. Available: http://www.multibandofdm.org/

[2] G.R. Aiello, G.D. Rogerson, "Ultra-Wideband Wireless Systems", IEEE Microwave Mag., pp. 36-47, June 2003.

[3] S. Roy, J.R. Foerster, V.S. Somayazulu, D.G Leeper, "Ultrawideband Radio Design: The Premise of High-Speed, Short Range Wireless Connectivity", Proc. of the IEEE, vol. 92, no. 2, pp. 295-311, Feb. 2004.

[4] A. Sibille, S. Bories, "Spatial diversity for UWB communications", 5th European Personal Mobile Communications Conference , EPMCC03, 22-25 April 2003, Glasgow, Scotland.

[5] "IEEE standard for information technology - telecommunications and information exchange between systems - local and metropolitan area networks - specific requirements part 15.3: wireless medium access control (MAC) and physical layer (PHY) specifications for high rate wireless

personal area networks (WPANs)", IEEE Std 802.15.3-2003, 2003, pp. 1-315.
[6] S.N. Makarov, Antenna and EM Modeling with MATLAB(r), Wiley-Interscience, 2002.
[7] D. Cassioli, M.Z. Win, A.F. Molisch, "The Ultra-Wide Bandwidth Indoor Channel: From Statistical Model to Simulations", IEEE J. on Selected Areas on Commun., vol. 20, no. 6, Aug. 2002, pp. 1247-1257.
[8] A.F. Molisch, J.R. Foerster, M. Pendergrass, M., "Channel models for ultrawideband personal area networks", IEEE Wireless Communications, vol. 10, no. 6, Dec. 2003, pp. 14 - 21.
[9] V. Hovinen, M. Hamalainen, T. Patsi, "Ultra wideband indoor radio channel models: preliminary results", 2002 IEEE Conference on Ultra Wideband Systems and Technologies, 2002. Digest of Papers. 21-23 May 2002, pp. 75-79.
[10] B. Vucetic, J. Yuan, Space-Time Coding, John Wiley and Sons, 2003.
[11] A. Hottinen, O. Tirkkonen, R. Wichman, Multi-antenna Transceiver Techniques for 3G and Beyond, John Wiley and Sons, 2003.
[12] W. C.-Y. Lee, Y.S. Yeh, "Polarization Diversity System for Mobile Radio", IEEE Trans. on Commun., vol. COM-20, no. 5, Oct. 1972, pp. 912-923.
[13] R.G. Vaughan, "Polarization diversity in mobile communications", IEEE Transactions on Vehicular Technology, vol. 39 , no. 3 , Aug. 1990, pp. 177-186.
[14] B. Lindmark, M. Nilsson, "On the available diversity gain from different dual-polarized antennas" IEEE Journal on Selected Areas in Communications, vol. 19, no. 2, Feb. 2001, pp. 287 - 294.
[15] C. Degen, W. Keusgen, "Performance evaluation of MIMO systems using dual-polarized antennas", 10th International Conference on Telecommunications ICT 2003, vol. 2, 23 Feb.-1 March 2003, pp. 1520-1525.
[16] S.M. Alamouti, "A simple transmit diversity technique for wireless communications", IEEE Journal on Selected Areas in Communications, vol. 16, no. 8, Oct. 1998, pp. 1451 - 1458.
[17] R. Van Nee, R. Prasad, Ofdm for Wireless Multimedia Communications, Artech House Pub., 2000.
[18] S. Hara, R. Prasad, Multicarrier Techniques for 4G Mobile Communications, Artech House Pub., 2003.
[19] A. Saleh, R. Valenzuela, "A Statistical Model for Indoor Multipath Propagation", IEEE J. on Selected Areas on Commun., vol. SAC-5, no. 2, Feb. 1987, pp. 128-137.
[20] IEEE 802.15 WPAN High Rate Alternative PHY Task Group 3a (TG3a) [Online]. Available: http://www.ieee802.org/15/pub/TG3a.html